NMR- and CD-Monitored Lipid-Binding Studies Suggest a General Role for the FATC Domain as Membrane Anchor of Phosphatidyl-Inositol-3 Kinase-Related Kinases (PIKKs)

Lisa A. M. Sommer[1], Martin Schaad[2], Sonja A. Dames[1$]

From the [1]Chair of Biomolecular NMR Spectroscopy, Department of Chemistry, Technische Universität München, Lichtenbergstr. 4, 85747 Garching, Germany, [2]Current Address Quintiles AG, Hochstrasse 50, CH-4053 Basel, Switzerland

[$]To whom correspondence may be addressed: Chair of Biomolecular NMR Spectroscopy, Department of Chemistry, Technische Universität München, Lichtenbergstr. 4, 85747 Garching, Germany, Tel.: +49-89-28913292, Fax: +49-89-28913869, E-mail: (sonja.dames@tum.de)

Running title: Role of PIKK FATC as membrane anchor

Supplementary Information

Fig. S1: Top: Charge distribution in the FATC domains of different human PIKKs. Negatively charged residues are colored red and positively charged ones blue. Bottom: Sequence conservation of the FATC domains of ATM, ATR, SMG1, and TRRAP illustrated by alignments of the respective sequences from different organisms. All sequence alignments were generated using the program ESPript (1). See also Fig. 1B.

Fig. S2: Amino acid sequences of the used hDNAPKfatc GB1 fusion proteins and NMR spectra of hDNAPK-gb1ent and of the GB1 tag with a factor Xa instead of a enterokinase site

(gb1xa). Top: Superposition of the ^{1}H-^{15}N-HSQC spectra of free ^{15}N-hDNAPKfatc-gb1ent (black) and ^{15}N-gb1xa (red). The resonance assignments that were derived based on the NMR spectra for hDNAPKfatc-gb1ent are indicated by the one-letter amino acid code and the sequence position. The amino acid sequences are shown below. The 56 residues of the GB1 domain are colored in red, the linking thrombin-enterokinase or thrombin-factor Xa sites and the C-terminal 33 residues of the human DNA-PKcs FATC domain (4096-4128 in full-length) in black. Residues corresponding to the thrombin cleavage site are additionally labeled with a black circle and these corresponding to the enterokinase cleavage site with a black asterisk. The small insert shows the spectral region containing the resonances for the tryptophan side chain amide protons.

Fig. S3: NMR-titration of ^{15}N-hDNAPKfatc with DPC (A) and a 4:1 mixture of DioctPA/DOPA (B). See also Fig. 2 A, B. In contrast to Fig. 2 the full ^{1}H-^{15}N-HSQC spectra including the region showing the tryptophan side chain amide are shown. The color-coding is indicated at the top of each plot.

Fig. S4: Evaluation of the influence of charged residues in the linking enterokinase (ent, DDDDK) or factor Xa (xa, IEGR) site on the interaction of the respective GB1-hDNAPKfatc fusion proteins with DPC micelles. A-B, Superposition of the ^{1}H-^{15}N HSQC spectra of the hDNAPKfatc-gb1ent and hDNAPkfatc-gb1xa in the presence of increasing amounts of DPC, respectively. The used DPC concentrations and the respective color coding are indicated to right side of each plot.

Fig. S5: Superposition of the ^{1}H-^{15}N-HSQC spectra of ^{15}N-hDNAPKfatc-gb1ent in the absence (black) and presence of <30 mM DMPC liposomes (red) or <60 mM DMPC liposomes (green). See also Fig. 2F.

Fig. S6: Chemical shift changes of hDNAPKfatc due the presence of high concentrations of DPC micelles (150 mM, Fig. 2D) or DihepPC/DMPC bicelles (Fig. 2E) as a function of the sequence position. The data was recorded using hDNAPKfatc-gb1ent. The chemical shifts of the nuclei of the micelle-immersed state have been assigned as described in the methods section. Assignments for residues of the bicelle-immersed form were adapted from those of the micelle-immersed where this was possible based on a comparison of the respective

spectra in Fig. 2 D and E. The average chemical shift change for the backbone amide nitrogen and proton Δδ(N,H)av for hDNAPKfatc due to the presence of DPC micelles or DihepPC/DMPC bicelles was calculated as $[(\Delta\delta_{HN})^2 + (\Delta\delta_N/5)^2]^{1/2}$.

Fig. S7: Supplementary NMR analysis of the interaction of selected human PIKK FATC domains with different membrane-mimetics. A) Superposition of ^{1}H-^{15}N-HSQC spectra of hATMfatc-gb1ent in the absence and presence of increasing amounts of DPC. The color coding and the respective DPC concentrations are given in the spectrum. To better identify the signals of the ATM FATC part, the spectrum of the GB1 tag (GB1-xa) is additionally shown in green on top. B) Superposition of the natural abundance ^{1}H-^{15}N-HSQC spectra of hSMG1fatc in the absence and presence of DihepPC micelles.

Fig. S8: Analysis of the interaction of the hATRfatc peptide with DPC micelles by 1D ^{1}H-NMR spectra. The spectrum of the free form is shown in blue, the one in the presence of 50 mM d_{38}-DPC in red. The top panel shows the full spectrum. The middle panel shows only the amide region. Here almost all signals arise from the protein. Only the sharp signal at about 7.6 ppm presumably arises from residual chloroform or another substance present in the DPC stock. The bottom panel shows part of the aliphatic region. Here, several signals from buffer substances are visible (see labels in the plot).

Fig. S9: The free isolated DNA-PKcs FATC domain is largely unstructured. The CD spectrum of hDNAPKfatc (top) shows a minimum around 200 nm typical for unstructured proteins and only a very weak minimum around 222 nm that usually together with a second minimum a 208 nm indicates the presence of α-helical secondary structure. This is consistent with the $^{13}C^{\alpha}$ secondary shifts measured for free hDNAPKfatc-gb1ent (Fig. 3) and the measured $^{1}H^{\alpha}$ shifts (not shown) and $^{3}J_{HNH\alpha}$ coupling constants (bottom) of hDNAPKfatc. The $^{3}J_{HNH\alpha}$ coupling constants were derived from a 3D HNHA spectrum (grey uncorrected, black corrected by 11% as suggested in the literature, see methods). Values below about 6-6.5 Hz are typically observed in α-helical regions, whereas values above about 8-8.5 Hz are characteristic for residues in β-sheets. Values in the range of about 6.5-8 Hz are typical for protein regions undergoing conformational exchange (see also methods).

Fig. S10: A-C, additional secondary shifts for micelle-immersed hDNAPKfatc based on data recorded using hDNAPKfatc-gb1ent. The $^{1}H^{\alpha}$-secondary shifts are similar to the $^{13}C^{\alpha}$-secondary shifts given in Fig. 4A sensitive to the adopted secondary structure (2). The $^{1}H^{N}$- and ^{15}N- secondary shift are not very sensitive to the particular secondary structure and were just plotted to show that the respective chemical shift values of the micelle immersed state deviate significantly from reported for random coil values (3). D, the shown table lists the presence of ^{1}H-^{1}H NOE-correlations typically observed in helical protein regions (4) for micelle-immersed hDNAPKfatc.

Fig. S11: Backbone dynamics of hDNAPKfatc-gb1ent in the free (A) and micelle-immersed state induced by the presence of 150 mM DPC (B), in each subfigure: ^{15}N-T_1 (top panel), ^{15}N -T_2 (middle panel) and $\{^{1}H\}$-^{15}N NOE values (bottom panel).

Fig. S12: Top two panels, additional secondary shifts for micelle-immersed hATMfatc to complement Fig. 4B. The $^{1}H^{N}$- and ^{15}N- secondary shift are not very sensitive to the particular secondary structure and were just plotted to show that the respective chemical shift values of the micelle immersed state deviate significantly from reported for random coil values (3). Bottom plot, $^{3}J_{HNH\alpha}$ values for micelle-immersed hATMfatc. For more explanations see legend of Fig. S9. The data was recorded using the construct hATMfatc-gb1ent.

Fig. S13: Analysis of changes in the backbone dynamics of hATMfatc-gb1ent upon interaction with DPC micelles based on $\{^{1}H\}$-^{15}N-NOE data. The data for the free form is shown in the top spectra, the one in the presence of DPC in the bottom ones. Positive peaks are colored black and red, negative peaks in blue and yellow. Each plot shows a superposition of the spectrum without (reference) and with NOE-effect. The plots to the right are the same as the ones to the left but show additionally the spectrum of the GB1 tag followed by factor xa site (gb1xa) in green on top to facilitate the identification of the peaks corresponding to the FATC part (no green peaks on top). For peaks corresponding clearly to the linker region (mostly in the more crowded central region) or the FATC part (for comparison see also the assigned spectra for hDNAPKfatc in Fig. 2 and SI Fig. S2) and that are labeled by numbers, the NOE-values have been determined and are displayed below. The assignments for the micelle-immersed ATM FATC domain are indicated by the one-letter amino acid code and the sequence position. For labels in brackets the NOE value is not given below. Since several

peaks of the free state of the ATM FATC domain are not visible, presumably due to motional averaging, which broadens them beyond detection, the respective chemical shift assignment was hampered.

1. Gouet, P., Courcelle, E., Stuart, D. I., and Metoz, F. (1999) *Bioinformatics* **15**(4), 305-308
2. Wishart, D. S., Sykes, B. D., and Richards, F. M. (1992) *Biochemistry* **31**(6), 1647-1651
3. Wishart, D. S., Bigam, C. G., Holm, A., Hodges, R. S., and Sykes, B. D. (1995) *J Biomol NMR* **5**(1), 67-81
4. Wüthrich, K. (1986) *NMR of proteins and nucleic acids*, Wiley-Interscience Publ., New York

Sommer et al., SI Fig. S1

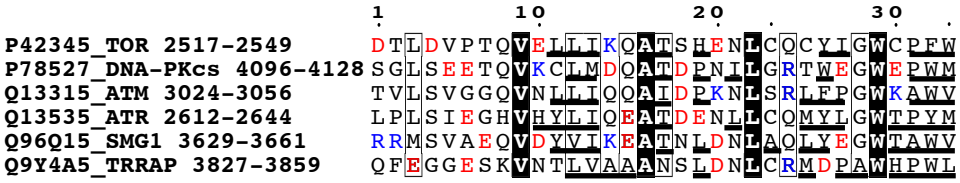

negatively charged/positively charged

ATM

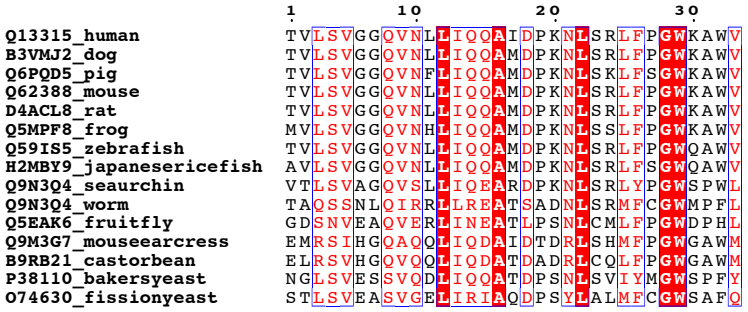

ATR

SMG1

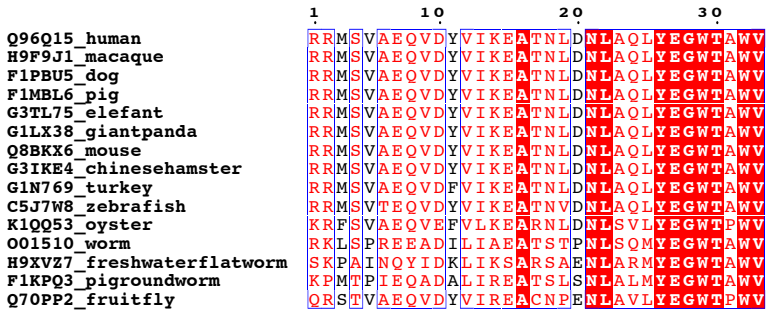

TRRAP

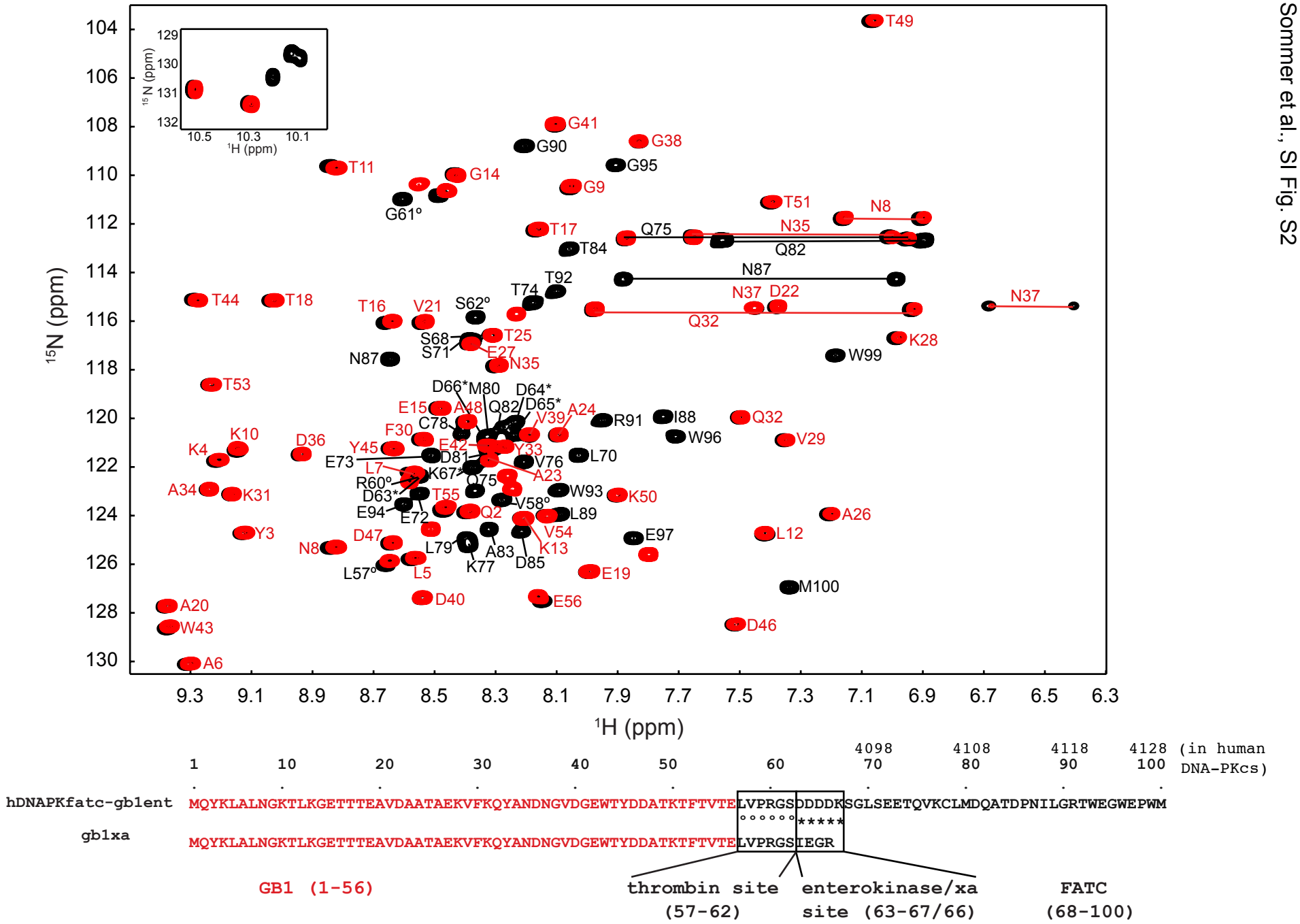

Sommer et al., SI Fig. S2

Sommer et al., SI Fig. S3

A Titration of hDNAPKfatc with DPC

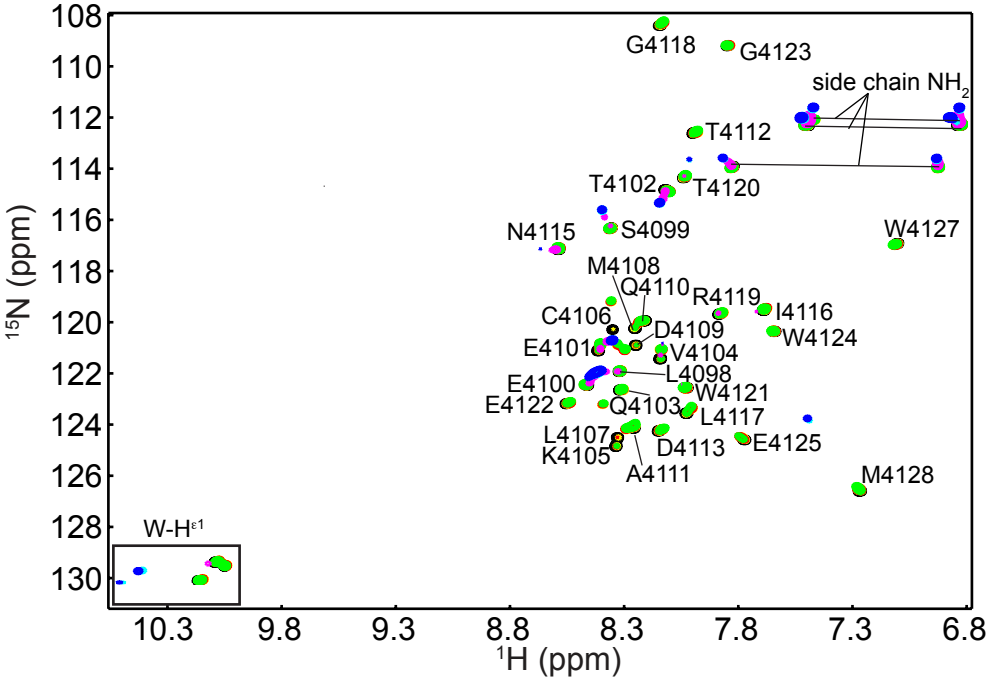

0 mM DPC
0.12 mM DPC
0.46 mM DPC
0.94 mM DPC
1.47 mM DPC
2.37 mM DPC
3.79 mM DPC

B Titration of hDNAPKfatc with DioctPA:DOPA

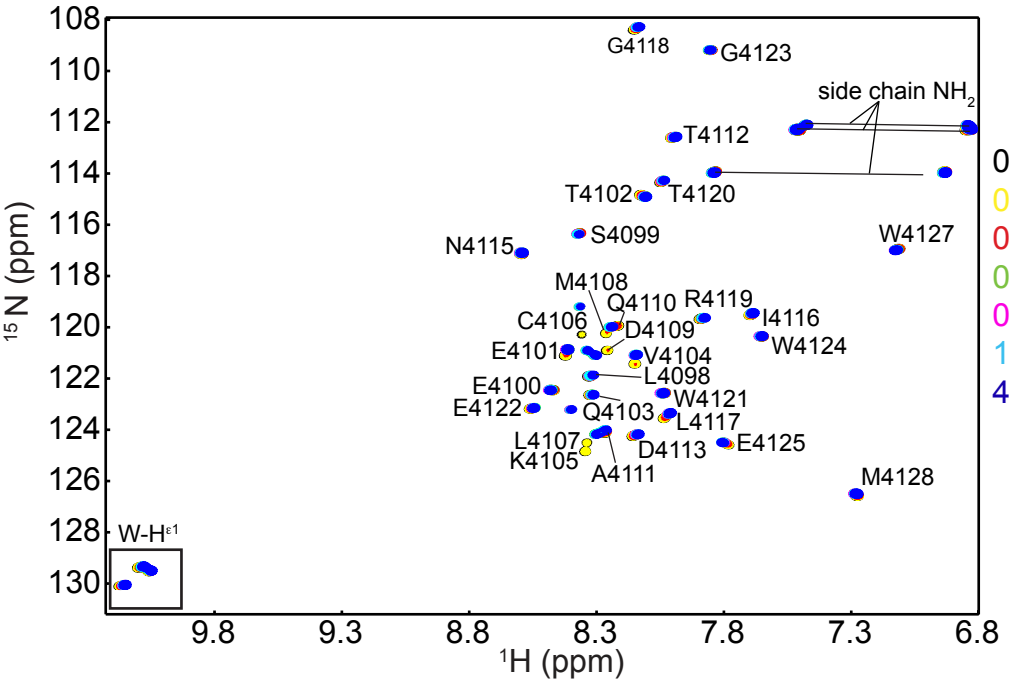

0 mM Dioct-PA:DOPA
0.06 mM Dioct-PA:DOPA
0.11 mM Dioct-PA:DOPA
0.22 mM Dicot-PA:DOPA
0.44 mM Dioct-PA:DOPA
1.12 mM Dicot-PA:DOPA
4.16 mM Dicot-PA:DOPA

Sommer et al., SI Fig. S4

A

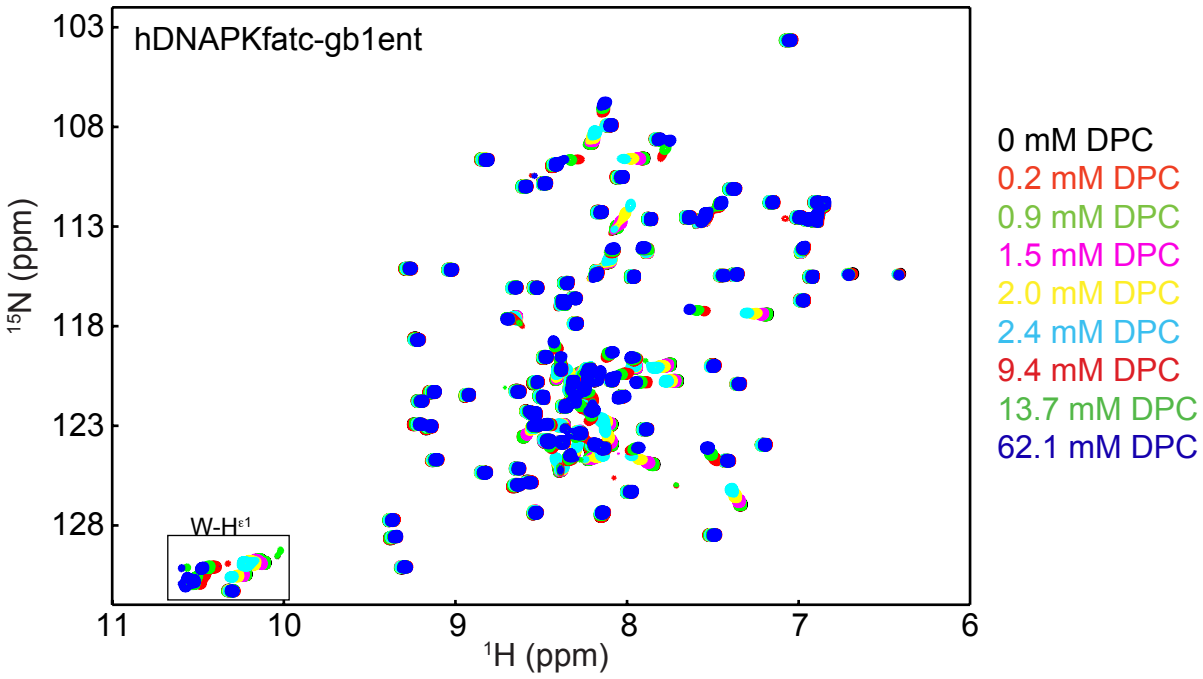

B

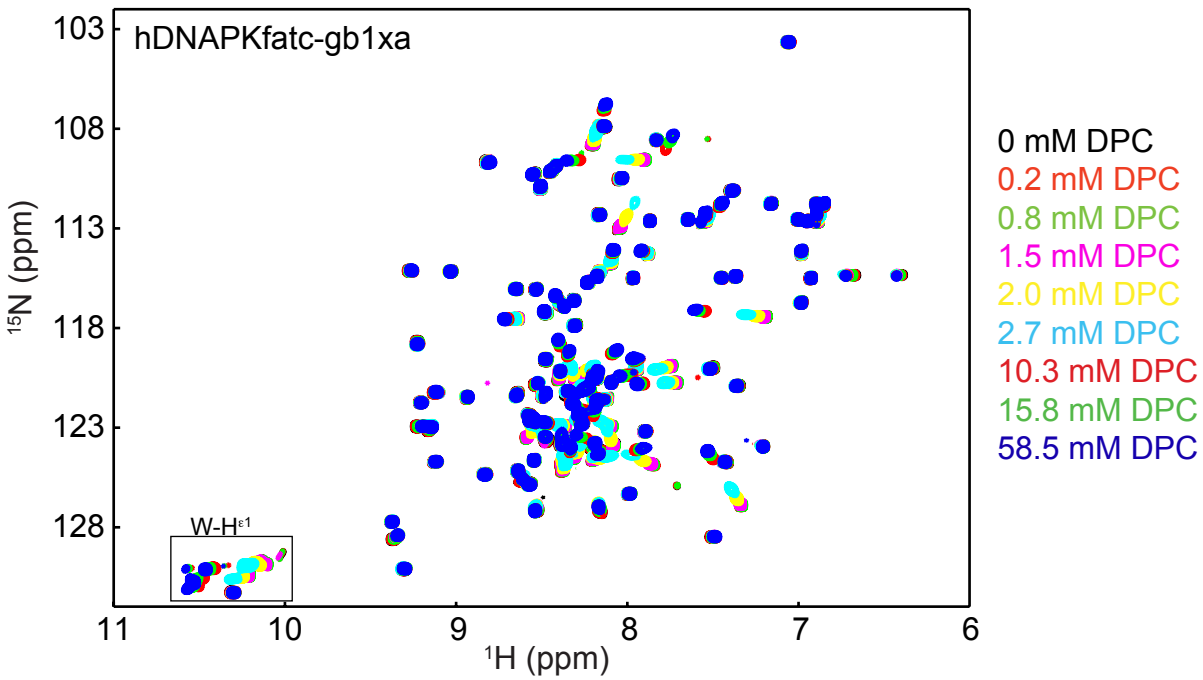

Sommer et al., SI Fig. S5

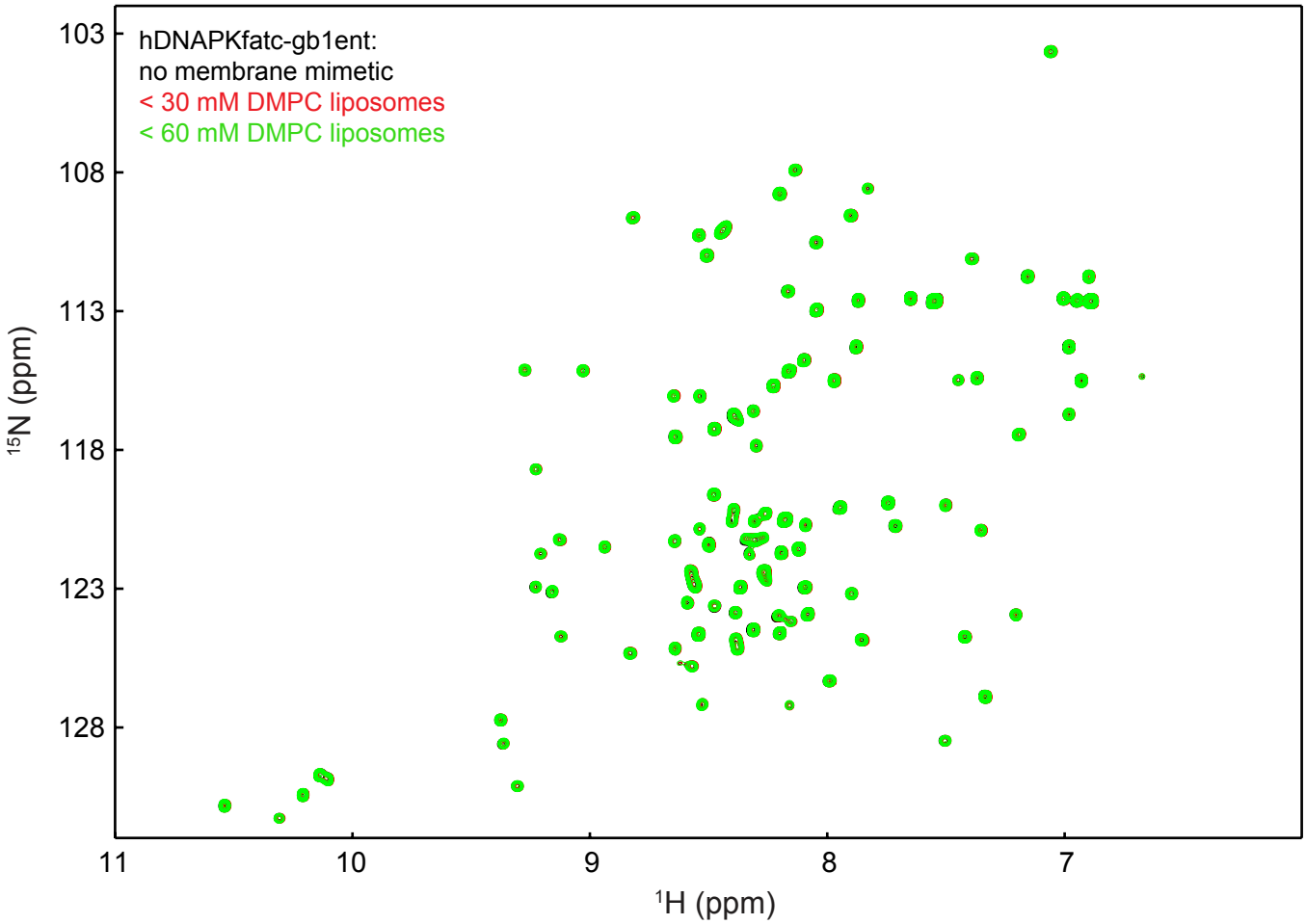

Sommer et al., SI Fig. S6

A Chemical shift changes for hDNAPKfatc due to DPC micelles (see Fig. 2D)

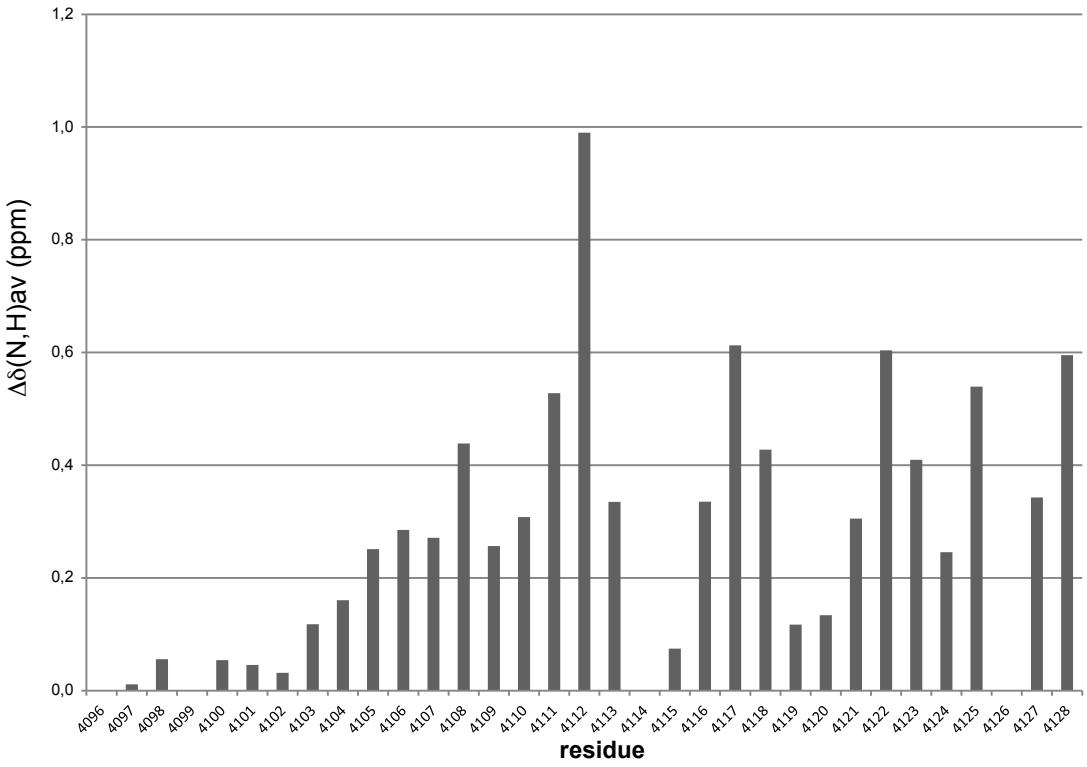

B Chemical shift changes for hDNAPKfatc due to Dihep-PC/DMPC bicelles (see Fig. 2E)

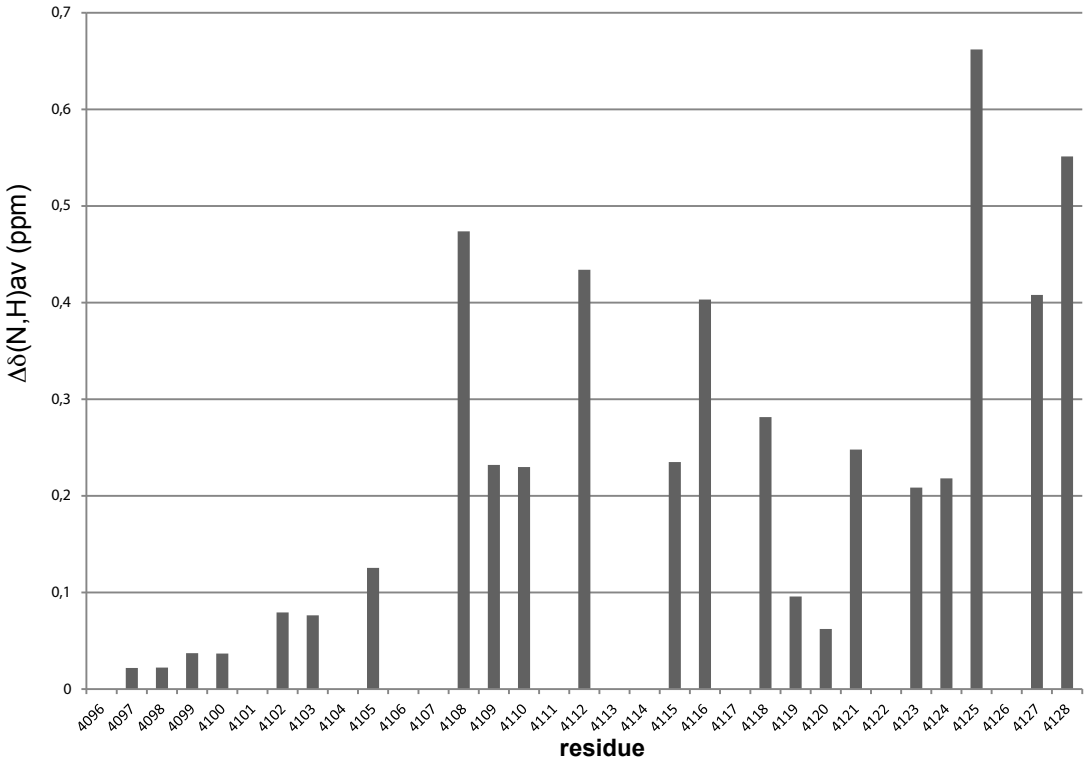

Sommer et al., SI Fig. S7

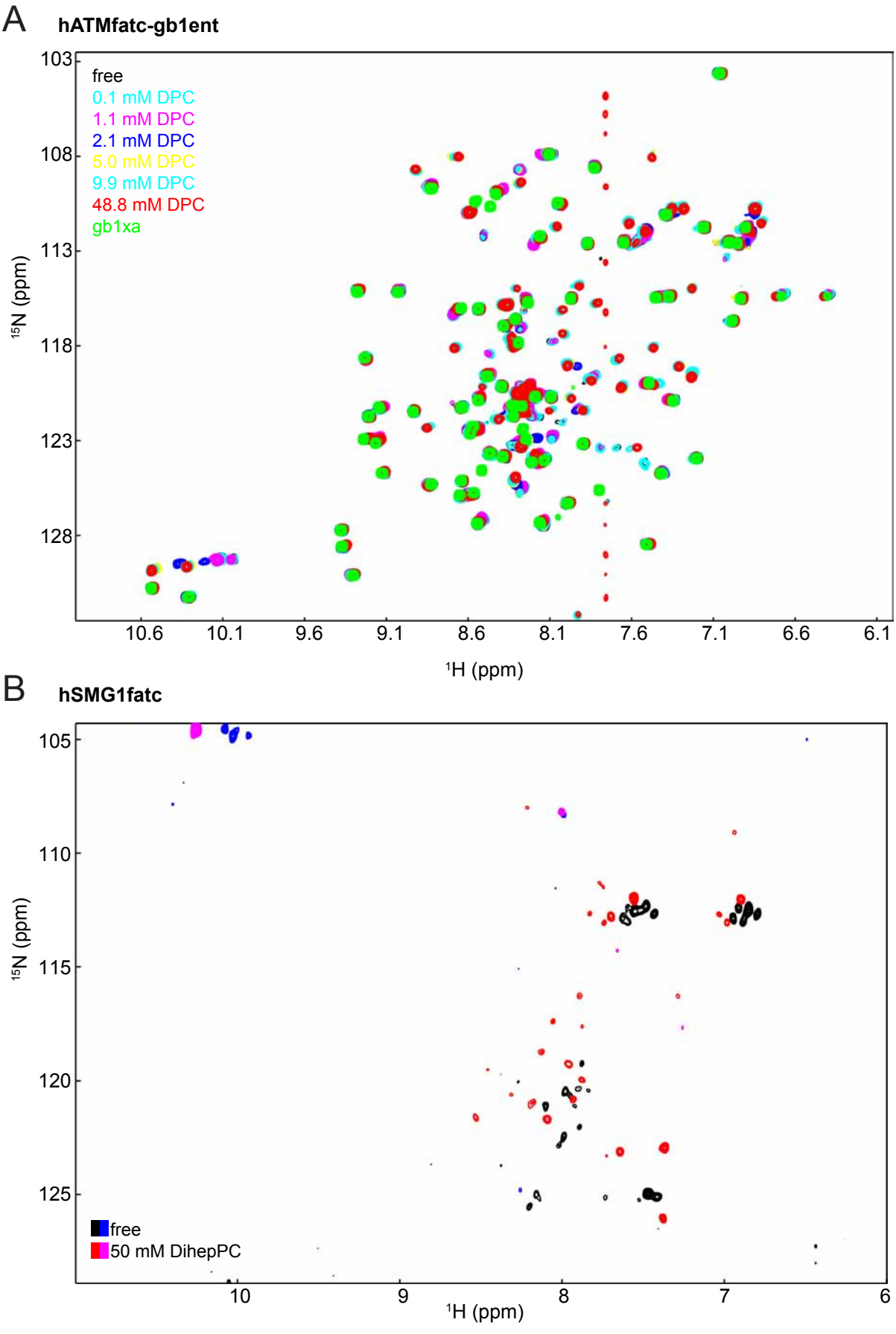

Sommer et al., SI Fig. S8

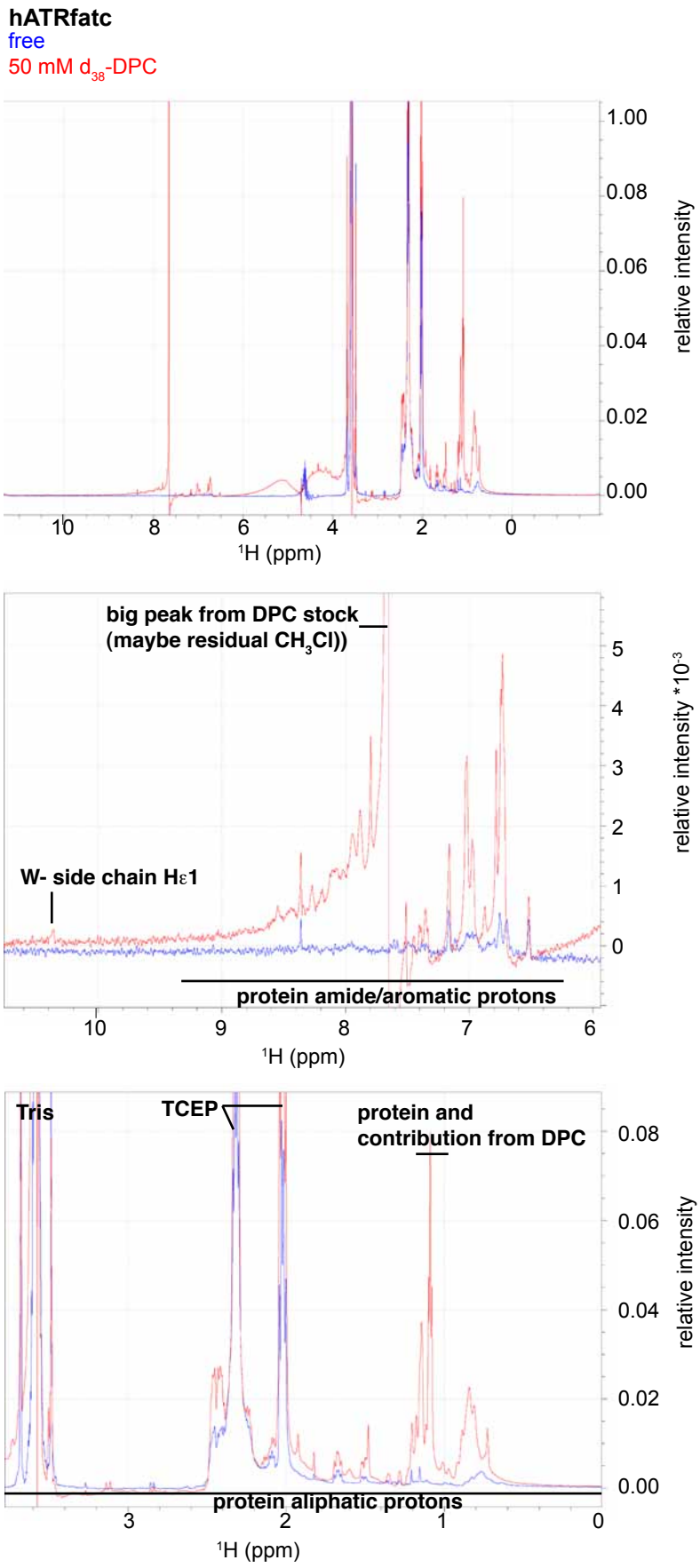

Sommer et al., SI Fig. S9

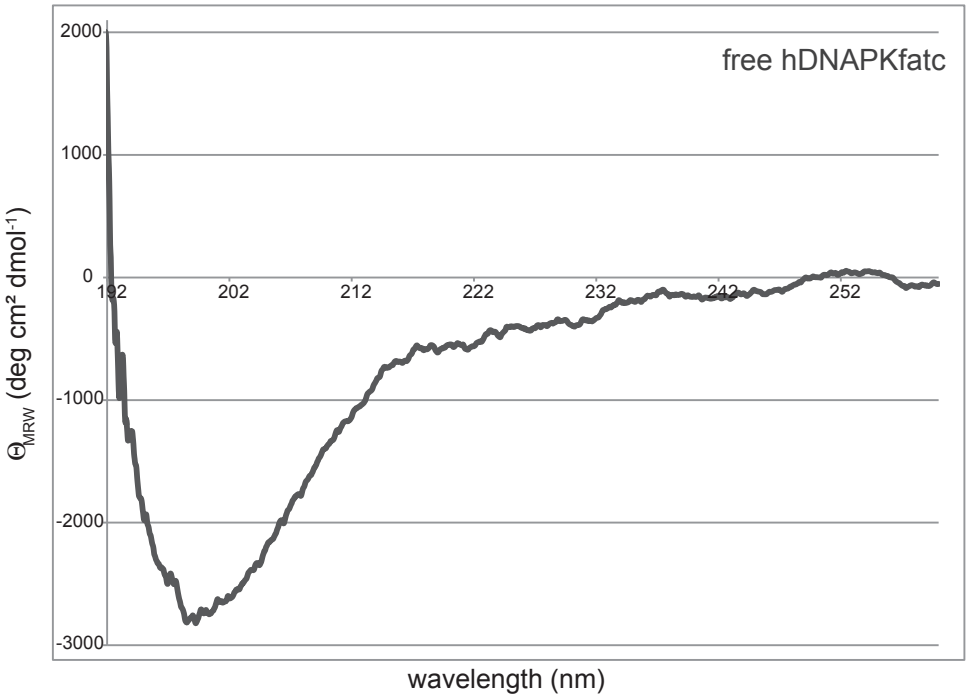

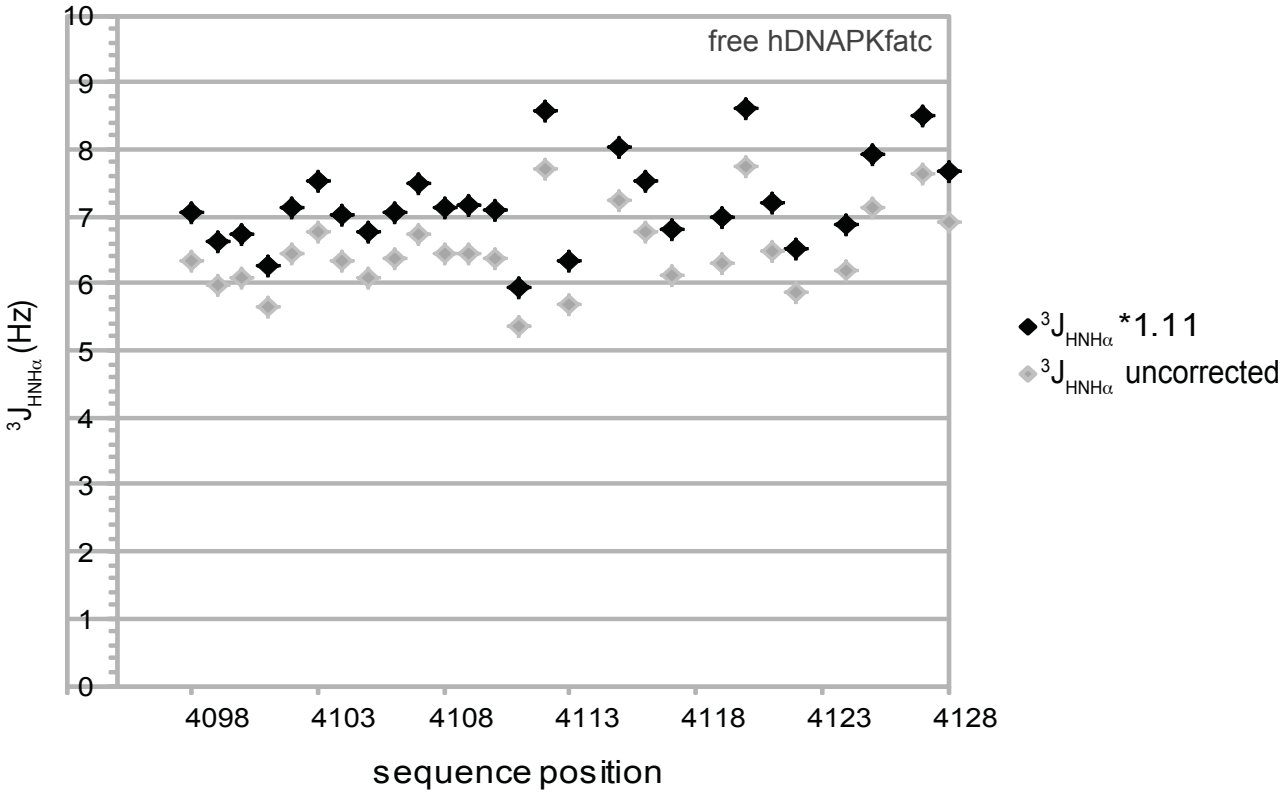

Sommer et al., SI Fig. S10

A

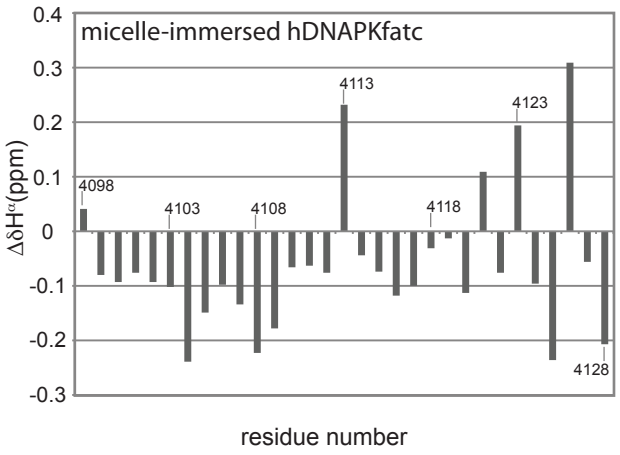

B

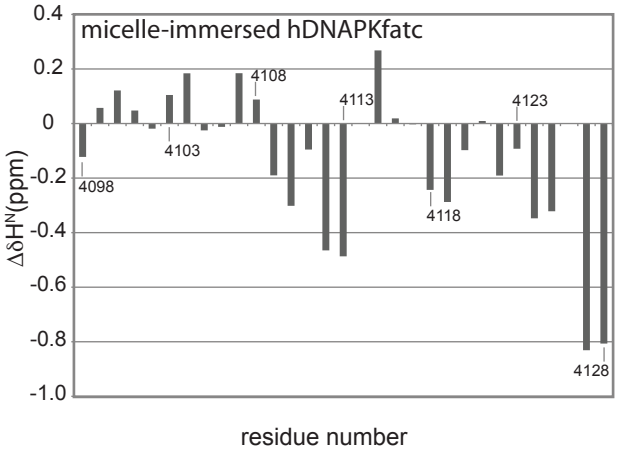

C

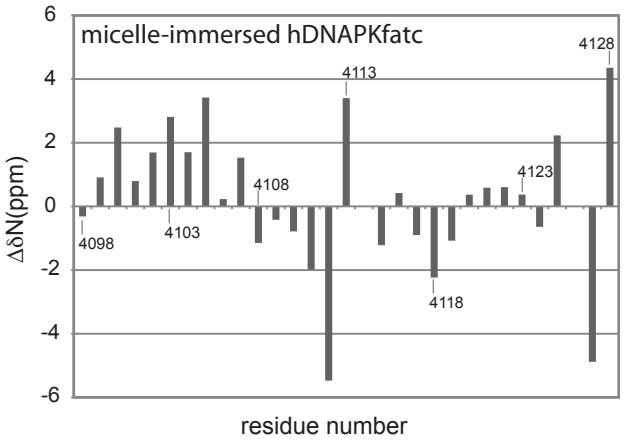

D micelle-immersed hDNAPKfatc

	4100	4101	4102	4103	4104	4105	4106	4107	4108	4109	4110	4111	4112	4113	4114
n, n i-1	+	+	++	++	++	(+)	(+)	(+)	++	(+)	++	++	++	++	x
n, n i+1	+	++	++	++	-	+	+	+	++	(+)	++	++	++	+	x
n, α i-3	x	(+)	-	+	-	+	-	(+)	-	++	-	++	++	+	x
n, α i-2	-	+	+	+	-	+	+	(+)	+	-	++	(+)	++	(+)	x
n, α i-4	x	x	-	-	-	+	-	+	+	(+)	-	-	++	-	x
n, α i-1	+	+	+	+	+	++	+	+	++	++	++	++	++	++	x

	4115	4116	4117	4118	4119	4120	4121	4122	4123	4124	4125	4126	4127	4128
n, n i-1	-	++	++	(+)	+	+	+	+	+	++	+	x	+	(+)
n, n i+1	++	+	(+)	(+)	(+)	+	+	(+)	++	+	-	x	(+)	x
n, α i-3	-	-	+	-	-	+	-	+	-	-	+	x	-	+
n, α i-2	++	-	(+)	(+)	(+)	-	-	+	-	-	-	x	+	-
n, α i-4	-	-	(+)	-	-	+	(+)	-	-	-	-	x	-	-
n, α i-1	++	++	(+)	+	+	+	+	(+)	-	+	-	x	(+)	+

++, strong; +, weak; (+), overlap

Sommer et al., SI Fig. S11

A free hDNAPKfatc-gb1ent

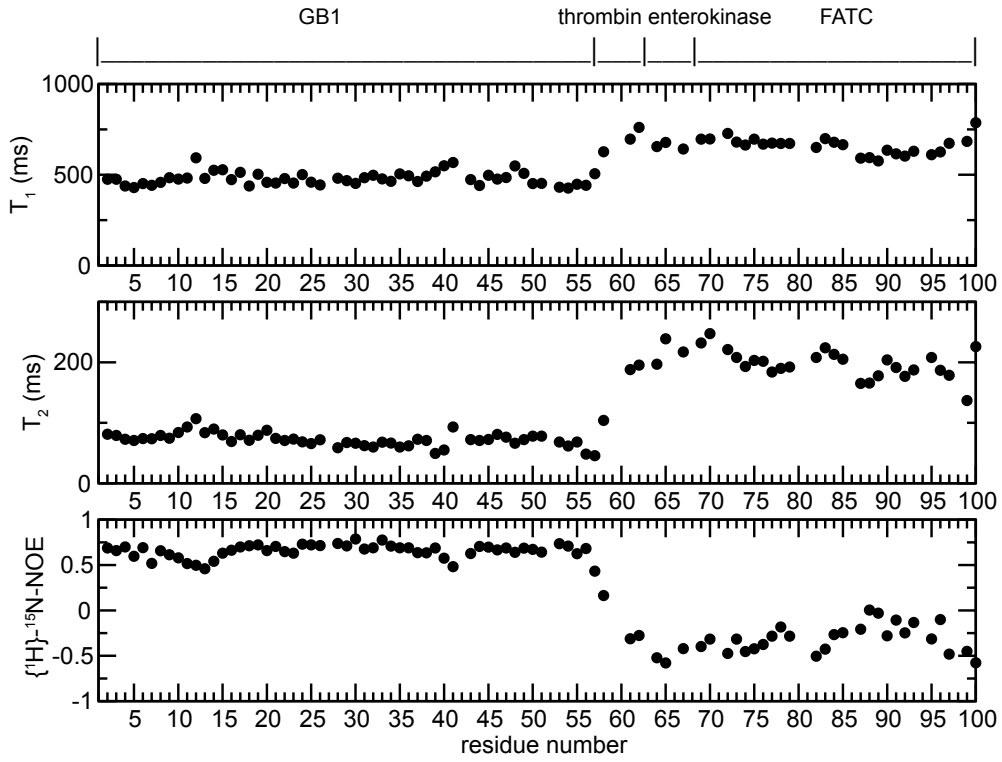

B micelle-associated hDNAPKfatc-gb1ent

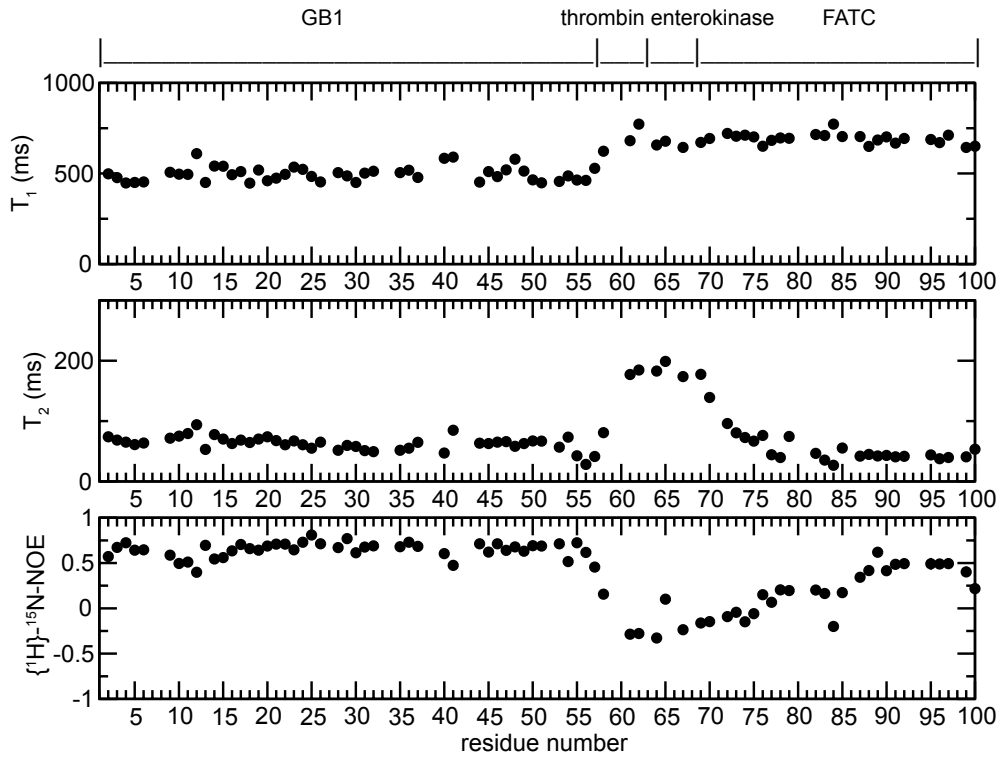

Sommer et al., SI Fig. S12

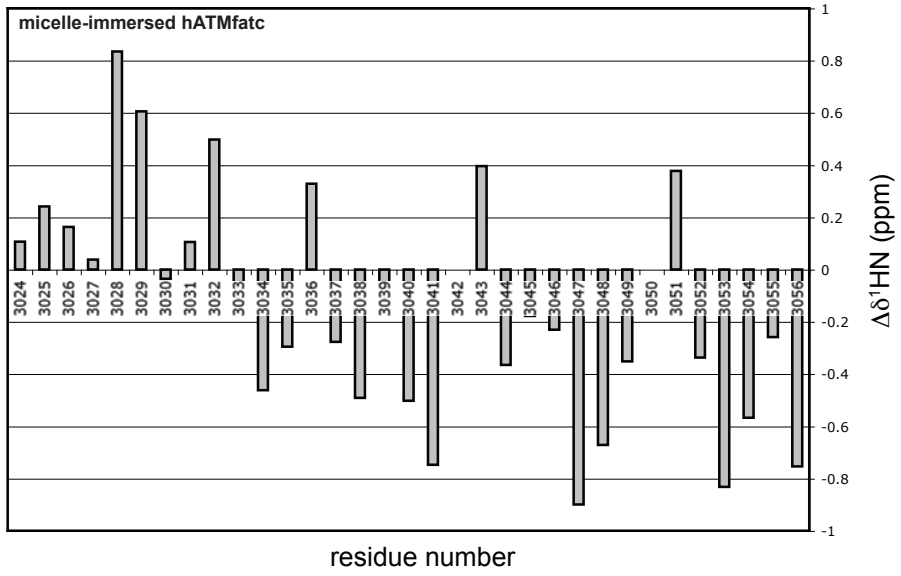

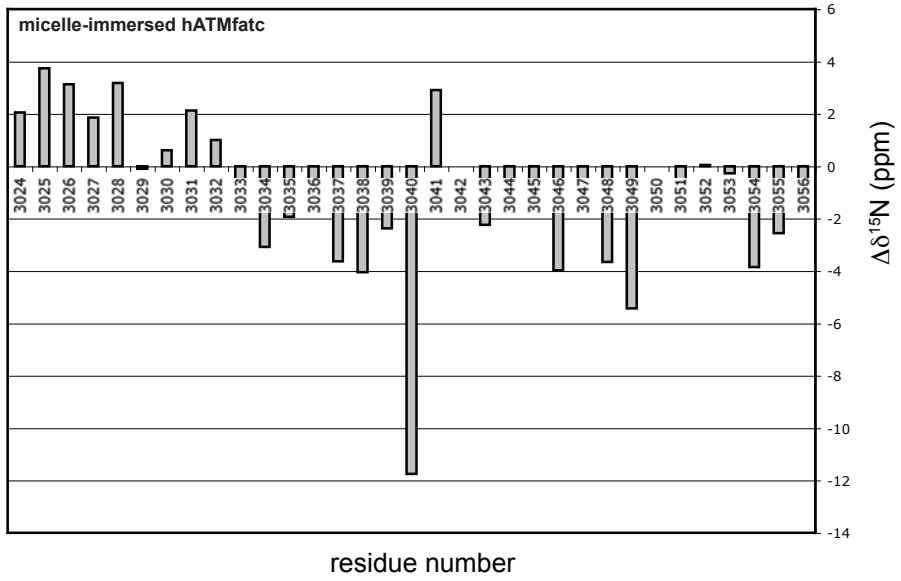

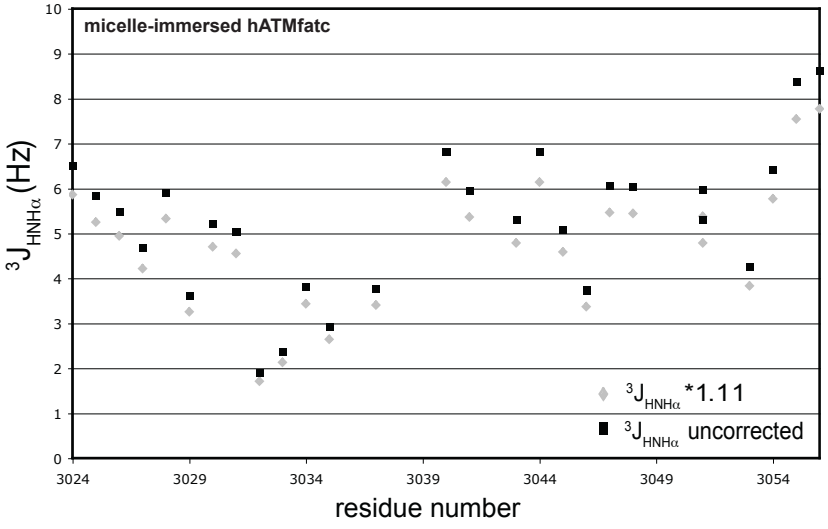

Sommer et al., SI Fig. S13

free hATMfatc-gb1ent

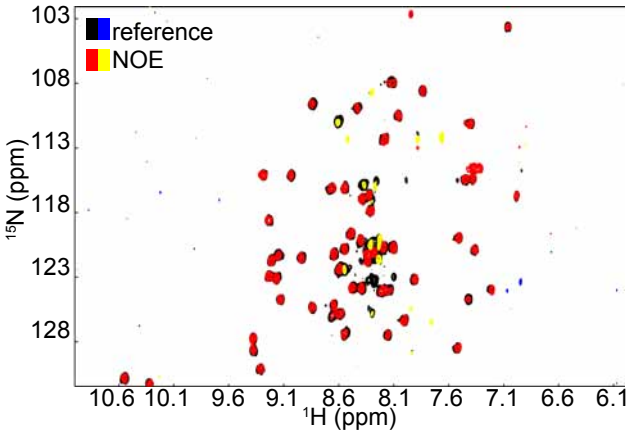

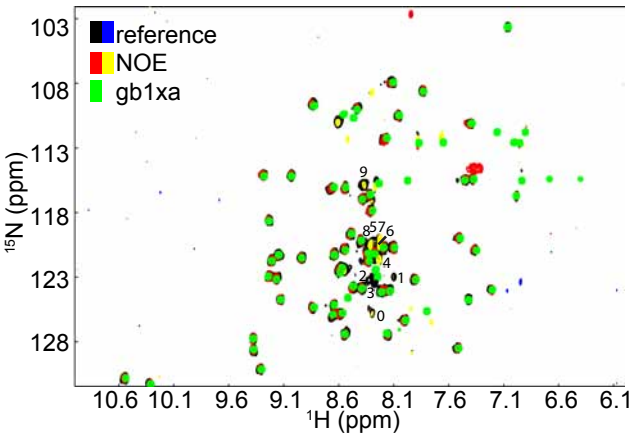

0	-0.56 ± 0.05	6	-0.34 ± 0.01
1	-0.45 ± 0.06	7	-0.55 ± 0.02
2	-0.09 ± 0.07	8	-0.44 ± 0.01
3	0.12 ± 0.02	9	-0.30 ± 0.02
4	-0.89 ± 0.03		
5	0.19 ± 0.06		

hATMfatc-gb1ent with 150 mM DPC

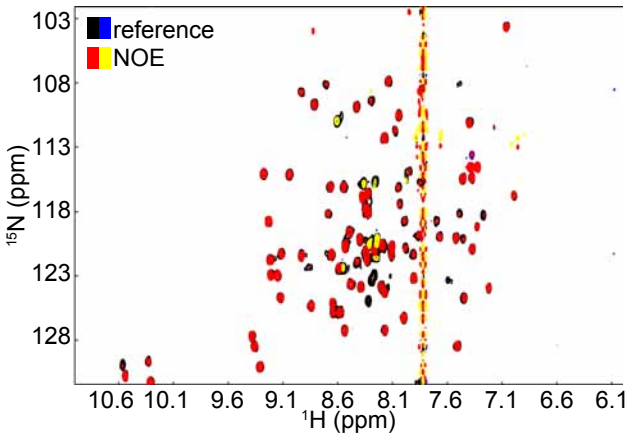

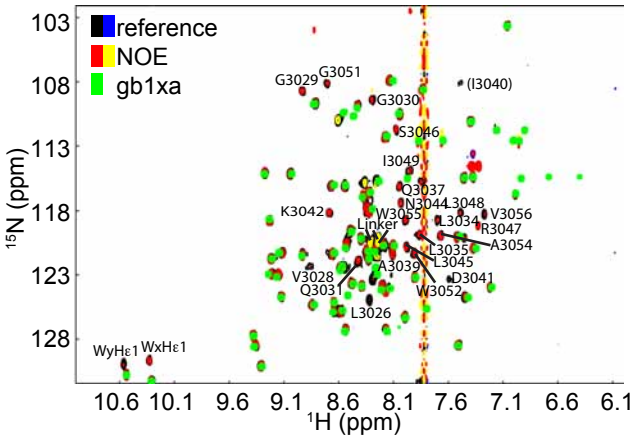

L3026	0.11 ± 0.02	D3041	0.32 ± 0.06	G3051	0.64 ± 0.05	Linker	-0.27 ± 0.01
V3028	0.55 ± 0.06	K2043	0.54 ± 0.03	W3052	0.72 ± 0.03	Linker	-0.42 ± 0.01
G3029	0.61 ± 0.04	N3044	0.56 ± 0.04	A3054	0.56 ± 0.02	Linker	-0.29 ± 0.01
G3030	0.57 ± 0.03	L3045	0.57 ± 0.04	W3055	0.48 ± 0.03		
Q3031	0.54 ± 0.03	S3046	0.52 ± 0.03	V3056	0.29 ± 0.03		
L3034	0.60 ± 0.05	R3047	0.73 ± 0.05	WxHε1	0.44 ± 0.02		
L3035	0.59 ± 0.04	L3048	0.42 ± 0.05	WyHε1	0.11 ± 0.01		
Q3037	0.68 ± 0.04	F3049	0.48 ± 0.04				
A3039	0.64 ± 0.03						